

# Opportunity Detection for OFDMA Systems with Timing Misalignment

Mustafa E. Şahin\*, Ismail Guvenc<sup>‡</sup>, Moo-Ryong Jeong<sup>‡</sup>, and Hüseyin Arslan\*

\*Dept. of Electrical Engineering, University of South Florida, Tampa, FL, 33620

<sup>‡</sup>DOCOMO Communications Laboratories USA, Inc., 3240 Hillview Avenue, Palo Alto, CA, 94304

Email: msahin@mail.usf.edu, {iguvenc, jeong}@docomolabs-usa.com, arslan@eng.usf.edu

**Abstract**— Accurate detection of spectrum opportunities within the frequency band of an orthogonal frequency division multiple access (OFDMA) system is a critical requirement for the realization of a coexisting cognitive radio. In this paper, we analyze the opportunity detection performances of energy detection and ESPRIT algorithms in the presence of timing misalignments in uplink (UL) OFDMA. For the energy detector, the statistics of subcarrier power are derived, and the accuracy of these derivations is verified through simulations. The feasibility of opportunity detection in an asynchronous UL-OFDMA system is proven. Also, it is shown that energy detection has a considerably better performance than the ESPRIT algorithm especially when the subcarrier assignments change frequently.

**Index Terms**— Cognitive radio, Femtocell, OFDMA, Opportunity Detection, Timing Misalignment.

## I. INTRODUCTION

Wireless standards through the last decade have mostly been using code division multiple access (CDMA) in their physical layers. For example, International Mobile Telecommunications-2000 (IMT-2000), which is the worldwide standard for third generation (3G) wireless technologies defined by the International Telecommunication Union (ITU), defines six standards for 3G networks, three of which are based on CDMA: Wideband CDMA, CDMA-2000, TD-CDMA/TD-SCDMA, EDGE, DECT, and WiMAX. While the first five of these standards were approved by ITU in 1999, WiMAX, which is based on orthogonal frequency division multiple access (OFDMA), was approved by the ITU in 2007.

OFDMA technology has a number of advantages over the other wireless technologies such as easily managing multiple access interference and narrowband interference, enabling dynamic channel allocation, and allowing simple channel equalization in frequency domain. Due to these desired features, it is very likely that next generation wireless technologies (e.g., those to be defined under the IMT-Advanced standard within the next few years) will be based on OFDMA.

An important problem that will be faced by future wireless systems is the crowding of the radio spectrum. Due to the increasing number of wireless technologies, future systems will need to coexist in the same spectrum. Cognitive radio is seen as a promising solution in this direction [1], [2]. Coupled with the OFDMA technology, cognitive radio systems can opportunistically utilize the spectrum (subcarriers) not occupied by other users in the network during a given time. This requires to reliably sense the spectrum opportunities

in order to minimize probability of false alarms (PFA) and probability of misdetections (PMD) [3].

After detecting the presence of a primary user, a threshold based detector such as in [4] can be employed for detecting the spectrum opportunities, where, appropriate selection of the threshold is critical for good detection performance. A particularly challenging scenario is when some of the uplink (UL) OFDMA user signals arrive at the receiver with delays larger than the cyclic prefix (CP) of the symbol (see e.g., [5]-[7]); this results in inter-symbol interference (ISI) as well as inter-carrier interference (ICI), and may considerably decrease the spectrum opportunities.

The coexistence of a femtocell network [8] with a macrocell network, both of which employ OFDMA, constitutes an interesting example where timing misalignment may occur. As discussed in [9], macrocell and femtocell may coexist through either a split-spectrum approach, where both networks are assigned orthogonal bands, or a shared-spectrum approach, where unused parts of the macrocell spectrum are utilized by the femtocell that acts as a cognitive radio. In a shared-spectrum scenario, while the macrocell users are synchronized with the macrocell base station (BS) through ranging, their signals may arrive at the femtocell BS with different delays, which can make detection of spectrum opportunities by the femtocell quite challenging.

In this paper, detection of spectrum opportunities in UL-OFDMA is investigated in the presence of timing misalignments between different users. In particular, two different detection techniques are evaluated: energy detection and the ESPRIT algorithm. For energy detection, both a noise-based threshold and a normalized threshold are considered for detection of occupied subcarriers in two different subcarrier assignment schemes. The contribution of the paper is two-fold. First, it is theoretically and technically proved that it is feasible to detect the spectrum opportunities in UL-OFDMA signals even if there is a synchronization error that exceeds the CP size. Second, it is shown that energy detection has a considerably better performance than the ESPRIT algorithm especially when the subcarrier assignments are changed frequently.

The rest of this paper is organized as follows. Section II provides the system model. Section III explains energy detection approaches employing noise-based threshold and normalized threshold in detail and provides summarized information about

the ESPRIT algorithm. Simulation results are presented in Section IV. Finally, Section V concludes the paper.

## II. OFDMA SYSTEM MODEL AND PROBLEM STATEMENT

### A. Signal Model

Consider an OFDMA system with  $N_u$  users with frequency synchronization simultaneously active in the uplink. The time domain signal at the transmitter of user  $i$  can be written as

$$x_i(t) = \sum_{m=-\infty}^{\infty} \sqrt{E_{\text{tx},i}} \frac{1}{N} \sum_{k \in \Gamma_i} X_i^{(m)}(k) e^{\frac{j2\pi k(t-mT_s)}{T}}, \quad (1)$$

where  $m$  is the symbol index,  $E_{\text{tx},i}$  is the total transmitted energy per symbol for user  $i$ ,  $k \in \Gamma_i$  is the subcarrier index,  $\Gamma_i$  is the set of subcarriers (of size  $1 \times N_i$ ) assigned to user  $i$  out of  $N$  total subcarriers, and  $X_i^{(m)}(k)$  is the data on the  $k$ th subcarrier and  $m$ th symbol of the  $i$ th user.  $T_s = T + T_{\text{cp}}$  is the total symbol duration, where  $T$  is the duration of the useful part of the symbol, and  $T_{\text{cp}}$  is the length of the CP. The time domain aggregate received signal is the superposition of the received signals from all the users, each of which traverses through a different multipath channel

$$y(t) = \sum_{i=1}^{N_u} \sqrt{E_{\text{rx},i}} \sum_{l=0}^{L_i-1} h_i^{(m)}(l) x_i(t - \tau_{l,i} - \tilde{\tau}_i) + w(t), \quad (2)$$

where  $E_{\text{rx},i}$  is the received energy per symbol for user  $i$ ,  $L_i$  denotes the total number of multipath components (MPCs),  $h_i^{(m)}(l)$  is the amplitude of the  $l$ th MPC for user  $i$ ,  $\tau_{l,i}$  is the delay of the  $l$ th MPC for user  $i$ ,  $\tilde{\tau}_i$  is the propagation delay experienced by user  $i$ , and  $w(t)$  denotes the additive white Gaussian noise (AWGN). Note that the average received energy per subcarrier for a user depends on  $N_i$ , and is given by  $E_{\text{sc},i} = E_{\text{rx},i}/N_i$ .

If we consider the sampled time domain signal transmitted by the  $i$ th user, (1) can be expressed as

$$x_i^{(m)}(n) = \sqrt{E_{\text{tx},i}} \sum_{k \in \Gamma_i} X_i^{(m)}(k) e^{\frac{j2\pi kn}{N}}, \quad -N_{\text{cp}} \leq n \leq N-1, \quad (3)$$

which is assumed to arrive at the receiver with a delay  $\tilde{d}_i = \lceil N\tilde{\tau}_i/T \rceil$ . Then, aggregate discrete-time received signal can be expressed as

$$y(n) = \sum_{i=1}^{N_u} y_i(n) + w(n) \quad (4)$$

$$y_i(n) = \sqrt{E_{\text{rx},i}} \sum_{l=0}^{L_i-1} h_i^{(m)}(l) \times \sum_{m=-\infty}^{\infty} x_i^{(m)}(n - D_{l,i} - m(N + N_{\text{cp}})), \quad (5)$$

where  $D_{l,i} = \lceil N\tau_{l,i}/T \rceil + \tilde{d}_i$ . If  $D_{l,i} \leq N_{\text{cp}}$ , it is easy to prove that the frequency domain signal for the  $k$ th subcarrier of user  $i$  is given by  $Y_i^{(m)}(k) = \sqrt{E_{\text{sc},i}} H_i^{(m)}(k) X_i^{(m)}(k) e^{-\frac{j2\pi k D_{l,i}}{N}}$ ,

where  $H_i^{(m)}$  is the discrete Fourier transform (DFT) of  $h_i^{(m)}$  [7]. This implies that the received symbol is only a phase rotated version of the transmitted symbol. On the other hand, if  $D_{l,i} > N_{\text{cp}}$ , the FFT window at the receiver will include signals from two consecutive symbols of the transmitted signal. As a consequence, this will result in inter-symbol interference as well as inter-carrier interference. Then, the received signal on the  $k$ th subcarrier of user  $i$  can be written as [7]<sup>1</sup>

$$Y_i^{(m)}(k) = \sqrt{E_{\text{sc},i}} \sum_{l=0}^{L_i-1} h_i^{(m)}(l) \left\{ S_{\text{des},i} + I_{\text{self},i} + I_{\text{other},i} \right\}, \quad (6)$$

where the desired signal, interference from the same subcarrier of the previous symbol, and the total interference from other subcarriers are respectively given as

$$S_{\text{des},i} = X_i^{(m)}(k) K_1(i) e^{-\frac{j2\pi k D_{l,i}}{N}} \quad (7)$$

$$I_{\text{self},i} = X_i^{(m-1)}(k) K_2(i) e^{-\frac{j2\pi k (D_{l,i} - N_{\text{cp}})}{N}} \quad (8)$$

$$I_{\text{other},i} = \frac{1}{N} \sum_{p \in \Gamma_i, p \neq k} \left[ \frac{1 - e^{\frac{j2\pi (p-k)(D_{l,i} - N_{\text{cp}})}{N}}}{1 - e^{\frac{j2\pi (p-k)}{N}}} \right] \times \left( -X_i^{(m)}(p) e^{-\frac{j2\pi p D_{l,i}}{N}} + X_i^{(m-1)}(p) e^{-\frac{j2\pi p (N_{\text{cp}} - D_{l,i})}{N}} \right), \quad (9)$$

where  $K_1(i) = \frac{N - D_{l,i} + N_{\text{cp}}}{N}$  and  $K_2(i) = \frac{D_{l,i} - N_{\text{cp}}}{N}$ . Then, the aggregate frequency spectrum is given by

$$Y^{(m)}(k) = \sum_{i=1}^{N_u} Y_i^{(m)}(k) + W(k), \quad (10)$$

$W \sim \mathcal{N}(0, \sigma^2 + j\sigma^2)$  is the DFT of  $w$ , where  $\sigma^2 = N_0/2$ .

### B. Subcarrier Assignment Schemes in Different Standards

In an OFDMA system, time-frequency resources are dynamically shared between users, exploiting channel variation in both frequency and time domains. The resource allocation, therefore, takes the form of one or more two-dimensional blocks, where each block is defined by  $N_{\text{symb}}$  consecutive OFDMA symbols in the time domain and  $N_{\text{sc}}$  consecutive subcarriers in the frequency domain. In the standards, the block is referred using different names; it is referred as resource block (RB) in LTE, while referred as tile or bin in WiMAX [10]-[12]. When multiple blocks constitute a resource allocation, those blocks may be either distributed or localized in the frequency domain so that frequency diversity or channel dependent scheduling can be appropriately exploited. Table I summarizes the uplink parameters for  $N_{\text{symb}}$  and  $N_{\text{sc}}$  that are used in the standards<sup>2</sup>.

<sup>1</sup>While related derivation of (6) is available in [7], it considers only blockwise allocation.

<sup>2</sup>PUSC: partial usage of subchannels, ASP: adjacent subcarrier permutation.

TABLE I  
THE UPLINK PARAMETERS USED IN LTE AND WiMAX STANDARDS.

	LTE	WiMAX		
		PUSC 1	PUSC 2	ASP
$N_{\text{symb}}$	7 (or 6)	3	3	$N$ ( $= 1, 2, 3, \text{ or } 6$ )
$N_{\text{sc}}$	12	4	3	$9 \times M$ (where $N \times M = 6$ )

### III. OPPORTUNITY DETECTION FOR OFDMA

#### A. Energy Detector Approach

In the energy detector approach, we consider the following decision variable and compare it with a threshold  $\xi$

$$P^{(m)}(k) = \left| Y^{(m)}(k) \right|^2 \underset{H_0}{\overset{H_1}{\geq}} \xi, \quad (11)$$

where hypothesis  $H_1$  implies that subcarrier  $k$  is occupied, and hypothesis  $H_0$  implies that it is not. When a binary phase shift keying (BPSK) modulation is used, the mean and the variance of the decision variable in (11) can be approximately<sup>3</sup> derived as  $E\{P^{(m)}(k)\} = \sum_i E\{P_i^{(m)}(k)\}$  and  $\text{Var}\{P^{(m)}(k)\} = \sum_i \text{Var}\{P_i^{(m)}(k)\}$ .  $E\{P_i^{(m)}(k)\}$  and  $\text{Var}\{P_i^{(m)}(k)\}$  are given in (12) and (13), respectively, where  $\tilde{\Gamma}_i = [\Gamma_i \ \Gamma_i]$  and

$$f_i(p, k) = \frac{1 - \cos\left(\frac{2\pi(p-k)(D_{i,i} - N_{\text{cp}})}{N}\right)}{1 - \cos\left(\frac{2\pi(p-k)}{N}\right)}. \quad (14)$$

The mean and variance of (11) for a three user scenario are plotted in Fig. 1, where the simulation parameters in Table II are used, and an AWGN channel is considered. While user-1's signal arrives at the receiver with a delay smaller than the CP,

<sup>3</sup>Some noise-cross-signal terms and cross-terms between different users are neglected in the derivation of  $\text{Var}\{P^{(m)}(k)\}$  for simplicity.

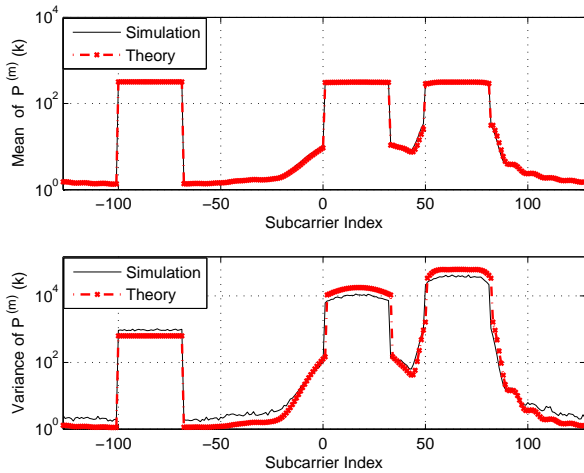


Fig. 1. Top: Simulation result and theoretical curve for the mean of the subcarrier power. Bottom: Simulation result and theoretical curve for the variance of the subcarrier power. User delays are  $\tilde{\tau}_1 = 10$ ,  $\tilde{\tau}_2 = 40$ ,  $\tilde{\tau}_3 = 60$ ; and subcarriers assigned to users are  $\Gamma_1 = [-100, -99, \dots, -69]$ ,  $\Gamma_2 = [1, 2, \dots, 32]$ ,  $\Gamma_3 = [50, 51, \dots, 81]$ , respectively.

user-2 and user-3's signals arrive at the receiver with delays larger than the CP. Fig. 1 shows that the power level of the subcarriers adjacent to the subcarriers of user-2 and user-3 are much larger than the noise level due to the propagation delay. Another important observation in Fig. 1 is that the variance of the decision variable at the occupied subcarriers of a certain user may increase considerably (e.g., on the order of 10 dB) with the delay experienced by that user.

For the detection of occupied subcarriers, we consider two types of thresholding techniques for selecting  $\xi$  in this paper: noise-based threshold (NBT) and normalized threshold (NT).

1) *Noise-based threshold*: If the noise variance  $\sigma^2$  is known, the threshold that satisfies a certain PFA can be selected. If subcarrier  $k$  is not occupied by any user, (11) follows a centralized Chi-square distribution, whose cumulative distribution function (CDF) is given by [13]

$$F_Y(y) = 1 - e^{-y/2\sigma^2} \sum_{\kappa=0}^{M-1} \frac{1}{\kappa!} \left(\frac{y}{2\sigma^2}\right)^\kappa, \quad (15)$$

where  $M = n/2$  is an integer, and  $n$  denotes the degree of freedom (DOF). For complex noise, we have  $n = 2$ , and (15) becomes the CDF of an exponential distribution. Then, the PFA becomes

$$P_{\text{fa}}(\xi) = 1 - F_Y(y) = \frac{\xi}{2\sigma^2} e^{-\xi^2/2\sigma^2}. \quad (16)$$

When subcarrier  $k$  is occupied, then (11) follows a non-centralized Chi-square distribution, whose CDF is given by [13]

$$\tilde{F}_Y(y, E_{\text{sc},i}) = 1 - Q_M\left(\frac{\sqrt{E_{\text{sc},i}}}{\sigma}, \frac{\sqrt{y}}{\sigma}\right), \quad (17)$$

where  $Q_M(a, b)$  is the Marcum-Q function given by

$$Q_M(a, b) = \int_b^\infty x \left(\frac{x}{a}\right)^{M-1} e^{-(x^2+a^2)/2} I_{M-1}(ax) dx, \quad (18)$$

with  $I_\alpha(x)$  denoting the  $\alpha$ th order modified Bessel function of the first kind [13]. Then, using (16), probability of detection  $P_d$  corresponding to a certain  $P_{\text{fa}}$  becomes

$$P_d(P_{\text{fa}}) = 1 - \tilde{F}_Y(\xi, E_{\text{sc},i}) = Q_M\left(\frac{\sqrt{E_{\text{sc},i}}}{\sigma}, \frac{\sqrt{F_Y^{-1}(1 - P_{\text{fa}})}}{\sigma}\right). \quad (19)$$

The relationship in (19) is commonly referred as the receiver operating characteristic (ROC) curves. The ROCs for a simple single-user scenario is illustrated in Fig. 2 for two different delays. When the propagation delay experienced by the user exceeds the CP, we observe that the probability of detection corresponding to a certain PFA may decrease considerably. Moreover, average error probabilities corresponding to different NTs are also plotted, which overlap with the NBT curves for the single-user scenario. Hence, by changing the NT values, a receiver may operate at different points on the ROC curves.

$$\mathbb{E}\{P_i^{(m)}(k)\} = \begin{cases} \frac{2E_{sc,i}}{N^2} \sum_{p \in \Gamma_i} f_i(p, k) + n\sigma^2, & \text{if } k \notin \Gamma_i, \\ \frac{2E_{sc,i}}{N^2} \sum_{p \in \Gamma_i, p \neq k} f_i(p, k) + n\sigma^2 + E_{sc,i}K_1^2(i) + E_{sc,i}K_2^2(i), & \text{if } k \in \Gamma_i, \end{cases} \quad (12)$$

$$\text{Var}\{P_i^{(m)}(k)\} = \begin{cases} \frac{8E_{sc,i}^2}{N^4} \sum_{\rho=1}^{2N_i-1} \sum_{\nu=\rho+1}^{2N_i} f_i(\tilde{\Gamma}_i(\rho), k) f_i(\tilde{\Gamma}_i(\nu), k) + 2n\sigma^4, & \text{if } k \notin \Gamma_i, \\ 4K_1^2(i)K_2^2(i)E_{sc,i}^2 + \frac{4E_{sc,i}^2}{N^2} (K_1^2(i) + K_2^2(i)) \sum_{p \in \Gamma_i, p \neq k} f_i(p, k) + 2n\sigma^4, & \text{if } k \in \Gamma_i, \end{cases} \quad (13)$$

2) *Normalized threshold*: Another convenient way of setting the threshold is to use a normalized threshold as follows

$$\xi = P_{\text{noise}} + T_{\text{norm}}(P_{\text{sn+noise}} - P_{\text{noise}}), \quad (20)$$

where  $P_{\text{noise}}$  and  $P_{\text{sn+noise}}$  denote the average noise energy and average signal+noise energy, respectively, and  $0 \leq T_{\text{norm}} \leq 1$  denotes the normalized threshold.

The noise energy can be estimated utilizing the guard bands (GB) of the OFDMA signal. By averaging the energies measured over the first half of the left GB and the second half of the right GB, an estimate that is affected least from the ICI can be obtained. The signal energy level can be roughly determined by averaging the energies measured over all subcarriers except the null subcarriers in the GBs.

### B. ESPRIT Algorithm

The problem of determining the occupied subcarriers of an OFDMA system can also be considered as identifying the number and frequencies of a set of sinusoids in additive noise. The ESPRIT method [14] handles this problem in time domain by making use of the shift invariance property of signals. OFDM signals are suitable for implementing ESPRIT because of their shift invariance thanks to the addition of the cyclic prefix; a time shift not exceeding the CP does not alter the statistical features of the signal. ESPRIT algorithm was proposed for estimating the occupied subcarriers of an

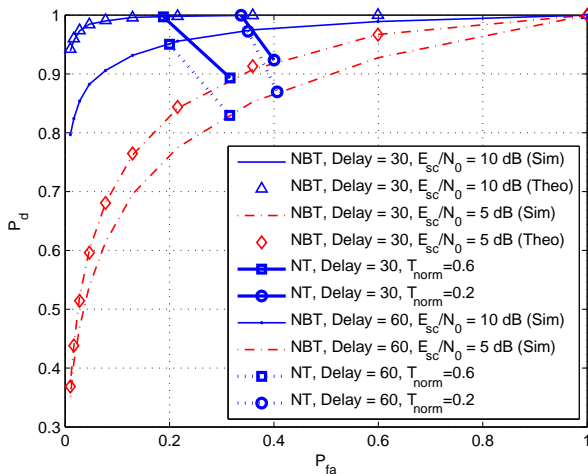


Fig. 2. The ROCs for a single-user scenario, where the simulation parameters in Table II are used and blockwise allocation is considered with  $\Gamma_1=[1,2,\dots,32]$ .

OFDM symbol in [15]. The estimation of the number of occupied subcarriers, which has a key importance for the ESPRIT performance, is accomplished through the minimum descriptive length (MDL) algorithm [16].

ESPRIT cannot be the optimum detection method when the maximum delay observed in the system is larger than CP due to the degradation in the shift invariance of OFDM symbols. In this paper, it is aimed to quantize the ESPRIT performance in an asynchronous UL-OFDMA system and to compare it with the energy detection performance.

## IV. SIMULATIONS

### A. Simulation Parameters

In the simulations, two different subcarrier assignment schemes are considered. The first one is a WiMAX UL ASP scheme with  $N=6$  and  $M=1$ . In the sequel, this scheme is referred as blockwise allocation (BA). The second scheme used, which we refer as randomized allocation (RA), allocates the subcarriers to users using a bin of a single subcarrier over 6 symbols. Although not used in any standard, the second scheme is included in our simulations to investigate the effect of using small number of subcarriers as an assignment unit. In the simulations corresponding to both schemes, the occupancy rate of the subcarriers is 50%.

A realistic 6-tap multipath (MP) channel (ITU-R Vehicular A channel model) is considered. The number of users is 12, and signal-to-noise-ratio (SNR) for user  $i$  is defined as  $\mathbb{E}\{E_{sc,i}\}/N_0$ . The maximum delay that the latest arriving user signal can have is  $\tau_{\text{max}}$ . In the simulations,  $\tau_{\text{max}}$  is considered to be between  $0 \mu\text{s}$  and  $60 \mu\text{s}$ , where  $\tilde{\tau}_i \sim \mathcal{U}(0, \tau_{\text{max}})$  for all users. Note that  $\tau_{\text{max}}$  values greater than  $11.2 \mu\text{s}$  exceed the CP duration. The remaining simulation parameters are listed in Table II.

### B. Simulation Results

In the simulations, the error probability is computed as the sum of PMD and PFA, where both probabilities are considered

TABLE II  
SIMULATION PARAMETERS

Parameter	Value
FFT Size	256
CP Size	1/8
Sampling frequency	2.857 MHz
Symbol Time	100.8 $\mu\text{s}$
CP Duration	11.2 $\mu\text{s}$
Bandwidth	2.5 MHz
Modulations	QPSK, 16QAM, 64QAM

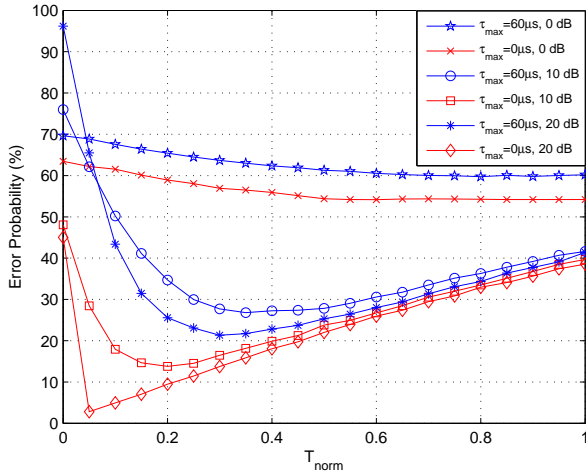


Fig. 3. Error probability vs. normalized threshold for blockwise allocation when  $\tau_{\max} = 0 \mu s$  and  $60 \mu s$  (for SNR = 20 dB, 10 dB, and 0 dB).

equally important. PMD is defined as the ratio of number of subcarriers detected as unused although they are used, to the number of used subcarriers. PFA, on the other hand, is the ratio of the number of subcarriers detected as used although they are unused, to the number of unused subcarriers.

The first analysis done on energy detection aims at determining the optimum  $T_{\text{norm}}$ . The error probability vs.  $T_{\text{norm}}$  curves are shown in Fig. 3 for BA. The curves that correspond to the lowest and highest  $\tau_{\max}$  values considered in the simulations ( $0 \mu s$  and  $60 \mu s$ ) are displayed for SNRs of 0 dB, 10 dB, and 20 dB, where all received user signals are assumed to have the same SNR. It is observed that, when SNR is high and  $\tau_{\max}$  is close to  $0 \mu s$ , the optimum  $T_{\text{norm}}$  is around 0.05, but a decrease in the SNR or an increase in  $\tau_{\max}$  gradually changes the optimum  $T_{\text{norm}}$  towards 0.5. Hence,  $T_{\text{norm}}$  may need to be set adaptively according to the SNR by utilizing the  $P_{\text{sn+noise}}$  and  $P_{\text{noise}}$  measurements.

The error probability vs.  $T_{\text{norm}}$  analysis is performed for different practical macrocell scenarios, as well. In these realistic simulations, received user signal powers are distance-dependent due to path loss. It is aimed to detect subcarriers of users whose average SNR exceeds 5 dB. Fig. 4 shows the error probabilities obtained for BA, where the distances of 12 users to the UL receiver are shown in the legend. The most critical observation in Fig. 4 is that the optimum  $T_{\text{norm}}$  is around 0.05 in all cases, which matches with the high SNR, low  $\tau_{\max}$  case in Fig. 3.

Fig. 5 demonstrates the error probability for  $\tau_{\max}$  values up to  $60 \mu s$  both for RA and BA. An optimum  $T_{\text{norm}}$  is used in all cases. It is observed that in RA, ICI has a more destructive effect on the detection performance. This is because in RA, each occupied subcarrier affects its adjacent subcarriers, some of which may be unoccupied. In the BA, however, the subcarriers that are strongly affected are limited to the ones that are adjacent to each block. Hence, the number of affected subcarriers is quite lower.

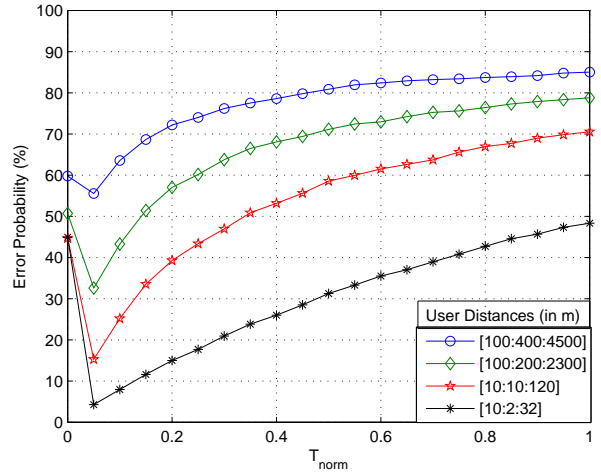


Fig. 4. Error probability vs. normalized threshold for 4 different macrocell scenarios.

The probability of error vs.  $\tau_{\max}$  analysis is performed for the ESPRIT algorithm, as well. From the results displayed in Fig. 6, it is observed that there is a considerable performance difference between RA and TA especially for high SNR values. For low SNRs, ESPRIT performance is considerably poor regardless of the subcarrier assignment scheme or the  $\tau_{\max}$  value.

A comparison of the error probabilities demonstrated in Fig. 5 and Fig. 6 indicates that the ESPRIT performance is inferior to the energy detection performance with the given set of simulation parameters. The main reason for this fact is that there are only 6 symbols over which the ESPRIT algorithm needs to obtain the autocovariance matrices it requires. It is found that ESPRIT performance could compete with energy detection only if the same subcarrier assignment were used over a very high number of symbols, so that ESPRIT can compute the autocovariances reliably. The simulation results that compare the performances of these two algorithms up to 500 symbols for RA, 20 dB SNR, and  $\tau_{\max} = 0 \mu s$  are plotted in Fig. 7. The energy detection curves are obtained for the optimum  $T_{\text{norm}}$  value for this scenario, which is 0.05, as well as two other non-optimum values. It is shown that ESPRIT can outperform energy detection at a high number of symbols, especially when  $T_{\text{norm}}$  is not optimized.

## V. CONCLUDING REMARKS

The feasibility of opportunity detection in UL-OFDMA with significant timing misalignments is investigated. Energy detection algorithm is scrutinized through detailed theoretical analysis and extensive simulations. Energy detector performance is found to be acceptable especially if the received signal power is high. ESPRIT algorithm has also been considered for detecting spectral opportunities. A comparison of the performances of the two algorithms showed that energy detection yields a better performance under the realistic system parameters considered.

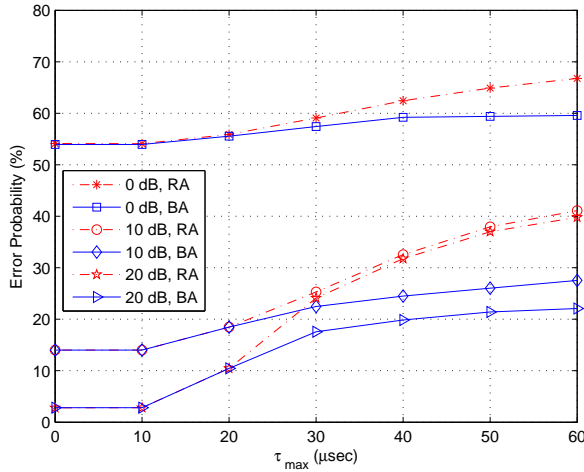


Fig. 5. Error probability vs.  $\tau_{\max}$  for energy detection with blockwise and randomized allocations.

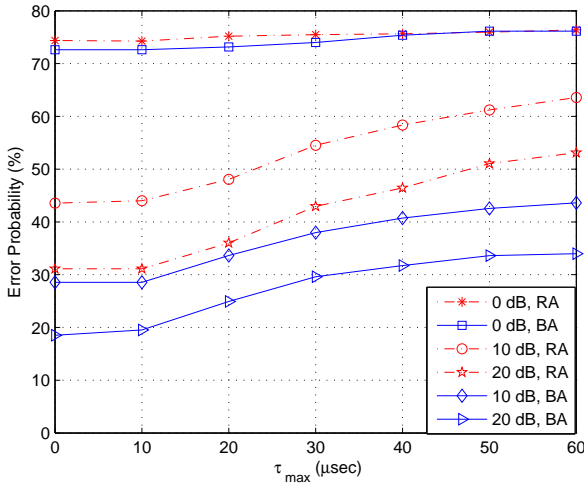


Fig. 6. Error probability vs.  $\tau_{\max}$  for the ESPRIT algorithm with blockwise and randomized allocations.

## REFERENCES

- [1] G. Ganesan and Y. G. Li, "Cooperative spectrum sensing in cognitive radio, part I: Two user networks," *IEEE Trans. Wireless Commun.*, vol. 6, no. 6, pp. 2204–2213, June 2007.
- [2] —, "Cooperative spectrum sensing in cognitive radio, part II: Multiuser networks," *IEEE Trans. Wireless Commun.*, vol. 6, no. 6, pp. 2214–2222, June 2007.
- [3] J. Hillenbrand, T. A. Weiss, and F. K. Jondral, "Calculation of detection and false alarm probabilities in spectrum pooling systems," *IEEE Commun. Lett.*, vol. 9, no. 4, pp. 349–351, Apr. 2005.
- [4] J. Ma and Y. G. Li, "Soft combination and detection for cooperative spectrum sensing in cognitive radio networks," in *Proc. IEEE Global Telecommun. Conf. (GLOBECOM)*, Washington, DC, Nov. 2007, pp. 3139–3143.
- [5] M. S. E. Tanny, Y. Wu, and L. Hazy, "OFDM uplink for interactive broadband wireless: Analysis and simulation in the presence of carrier, clock, and timing errors," *IEEE Trans. Broadcasting*, vol. 47, no. 1, pp. 3–19, Mar. 2001.
- [6] M. Park, K. Ko, H. Yoo, and D. Hong, "Performance analysis of OFDMA uplink systems with symbol timing misalignment," *IEEE Commun. Lett.*, vol. 7, no. 8, pp. 376–378, Aug. 2003.

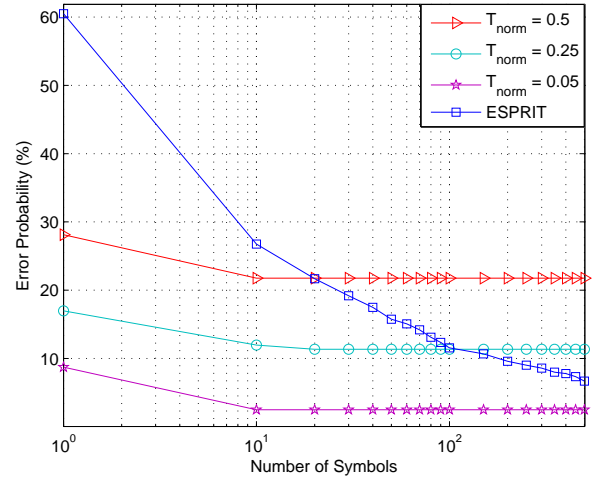


Fig. 7. Comparison of ESPRIT and energy detection algorithms over increasing number of symbols.

- [7] E. Bala and L. J. Cimini, "On the uplink synchronization of OFDMA systems," in *Proc. IEEE Military Commun. Conf. (MILCOM)*, Atlantic City, NJ, Oct. 2005, pp. 1133–1139.
- [8] Airvana, "Femto cells: Personal base stations," 2007, white Paper. [Online]. Available: [http://www.airvana.com/files/Femto\\_Overview\\_Whitepaper\\_FINAL\\_12-July-07.pdf](http://www.airvana.com/files/Femto_Overview_Whitepaper_FINAL_12-July-07.pdf)
- [9] V. Chandrasekhar and J. G. Andrews, "Uplink capacity and interference avoidance for two-tier cellular networks," in *Proc. IEEE Global Telecommun. Conf. (GLOBECOM)*, Washington, DC, Nov. 2007, pp. 3322–3326.
- [10] "3rd generation partnership project; technical specification group radio access network; evolved universal terrestrial radio access (E-UTRA); physical channels and modulation (release 8)," 3GPP, 3GPP TS 36.211, April 2008.
- [11] "IEEE standard for local and metropolitan area networks. part 16: Air interface for fixed broadband wireless access systems," IEEE Std 802.16-2004, Oct. 2004.
- [12] "IEEE standard for local and metropolitan area networks. part 16: Air interface for fixed and mobile broadband wireless access systems; amendment 2: Physical and medium access control layers for combined fixed and mobile operation in licensed bands," IEEE Std 802.16e-2005, Dec. 2005.
- [13] J. G. Proakis, *Digital Communications*, 4th ed. New York: McGraw-Hill, 2001.
- [14] R. Roy, A. Paulraj, and T. Kailath, "ESPRIT— A subspace rotation approach to estimation of parameters of cisoids in noise," *IEEE Trans. Acoust., Speech, and Signal Process.*, vol. 34, no. 5, pp. 1340–1342, Oct. 1986.
- [15] T. Yucek, "Channel, Spectrum, and Waveform Awareness in OFDM-Based Cognitive Radio Systems," Ph.D. dissertation, University of South Florida, 2007.
- [16] M. Wax and T. Kailath, "Detection of signals by information theoretic criteria," *IEEE Trans. Acoust., Speech, and Signal Process.*, vol. 33, no. 2, pp. 387–392, 1985.